

IFSCC 2025 full paper (IFSCC2025-886)

“Stress-Induced Hair Greying Modeled Using Human Hair-Bearing Organoids: A Step Toward a Sustainable Future”

Seoyeon Kyung¹, Su Jin Lim², Kyung Eun Lee¹, Yong il Kim², Hyun mun Kim², Noviana Wulansari², and Seunghyun Kang¹

¹ Affiliation 1; COSMAX BTI R&I Center

² Affiliation 2; Organoidsciences

1. Introduction

Hair greying is not merely a superficial sign of aging—it represents one of the earliest visible biological scars left by stress on the human body. Despite extensive research over the past several decades, the core mechanisms underlying stress-induced pigment loss in humans remain poorly understood, largely due to the field's continued reliance on non-human model systems. Historically, more than 100 million animals are sacrificed globally each year in the name of biomedical advancement [1], with countless lives devoted to a wide range of research areas including drug development, aging research, and cosmetic safety evaluation. While groundbreaking murine studies have linked sympathetic nervous system activation to melanocyte stem cell (McSC) depletion and irreversible hair greying [2], translating these findings to human biology has posed a persistent challenge.

In response to the critical demand for sustainable, human-relevant research models, we established a next-generation experimental platform through the generation of human pluripotent stem cell (hPSC)-derived hairy skin organoids, capable of faithfully modeling stress-induced hair greying. These organoids recapitulate not only the architecture of hair follicles but also the dynamic regulation of melanocyte populations under neuroendocrine stress. Using this model, we sought to mechanistically validate and expand upon prior findings that implicated NE in the premature depletion of McSCs and ectopic melanin deposition—phenomena that had previously only been validated in animal models [2]—now demonstrated for the first time in a physiologically relevant human system.

Using a multi-layered experimental design integrating morphological analysis, immunostaining, and single-cell RNA sequencing, we established framework capturing both structural and transcriptional alterations induced by NE induced stress. This approach revealed key features of stress-induced pigmentation loss, including premature melanocyte differentiation, pigment mislocalization, and impaired intercellular signaling. The use of a human-derived organoid system not only enhances the physiological relevance of our findings but also offers an ethical and sustainable alternative to animal testing—establishing a versatile platform not only for investigating pigmentation biology but also for modeling broader skin pathologies and accelerating personalized therapeutic innovation.

2. Materials and Methods

Human skin organoids were generated from hPSCs and cultured for 80 days to form hair follicle-like structures. Chronic stress conditions were modeled by treating the organoids with varying concentrations of NE for an additional 30 days. Morphological changes, including pigmentation and hair structure alterations, were evaluated via optical microscopy and histological staining.

Cryosections were analyzed through immunohistochemistry for markers related to extracellular matrix, melanogenesis, and smooth muscle integrity. For molecular profiling, scRNA-seq was conducted on organoids before and after NE treatment. Cell populations were clustered and annotated, followed by trajectory and pseudotime analysis. Intercellular communication networks were inferred using CellChat analysis, with a focus on signaling pathways implicated in pigmentation.

3. Results

3.1 NE Induces Ectopic Pigmentation and Alters Melanin Localization in Human Hairy Skin Organoids

To investigate stress-induced pigmentation, human hairy skin organoids were exposed to varying concentrations of NE. Bright-field images showed a dose-dependent increase in surface pigmentation, which was further emphasized in background-subtracted images highlighting melanin accumulation in the epidermis (Figure 1A, 1B). Tissue analysis revealed that, unlike the controls where melanin was localized near the hair bulb, NE-treated organoids showed ectopic melanin deposition in the epidermal layer (Figure 1C).

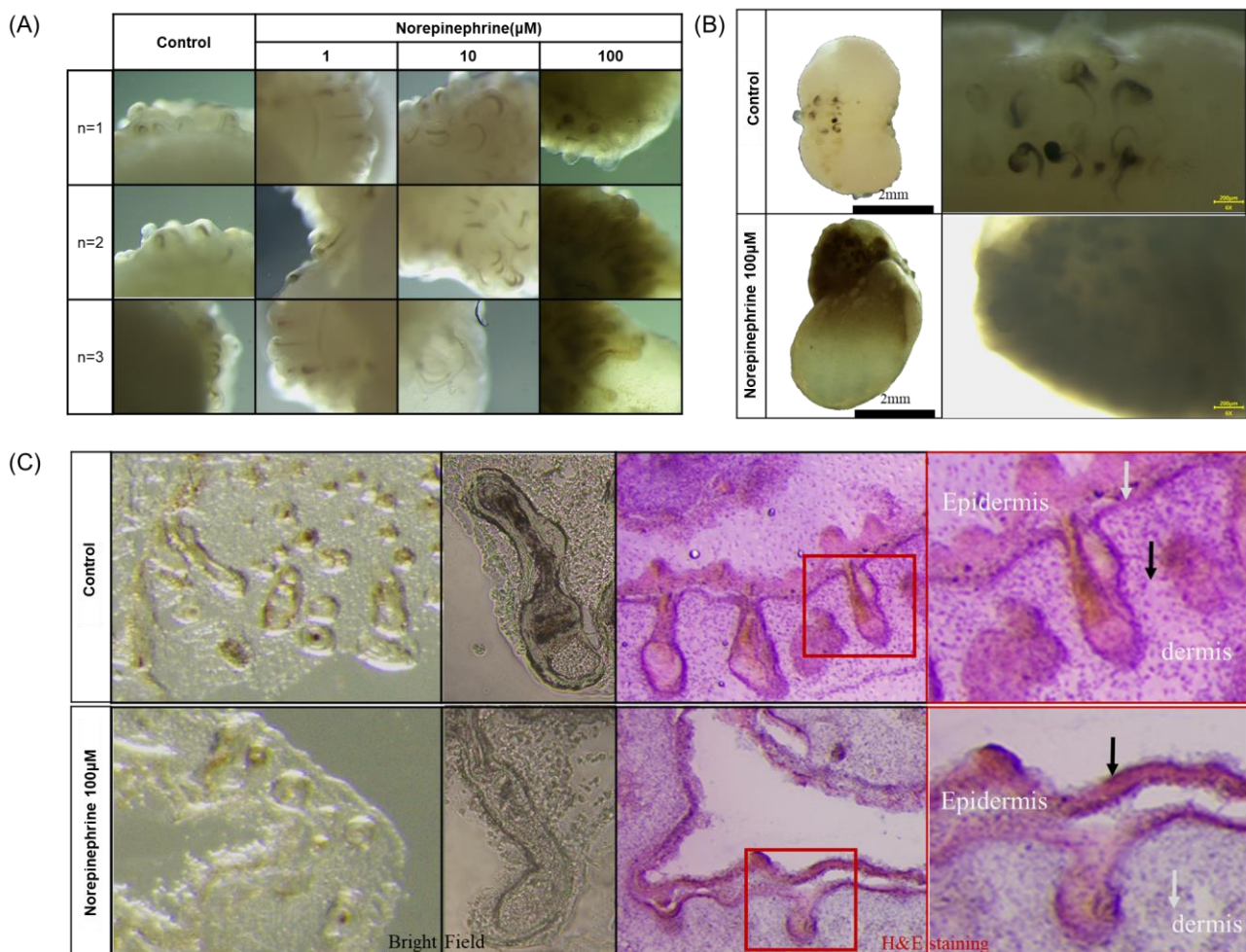


Figure 1. NE Induces Ectopic Pigmentation in Human Hairy Skin Organoids. (A) Representative bright-field images showing dose-dependent ectopic pigmentation on the surface of human hairy skin organoids upon NE treatment. (B) Background-removed images of whole organoids before and after NE exposure, highlighting surface pigmentation in NE-treated groups. (C) Bright-field and hematoxylin and eosin (H&E)-stained histological sections of hair follicle-containing regions.

3.2 NE Reduces Melanin Content in Hair Shafts and Depletes Stem and Pigment Cell Populations around Hair Root

To assess the functional consequences of stress on melanin synthesis observed at the tissue level, we further examined its impact at the hair shaft level by isolating individual fibers from organoids subjected to NE treatment. A carefully controlled dissection protocol was used to obtain intact hair shafts from both control and NE-exposed organoids (Figure 2A). High-resolution microscopy revealed a marked reduction in pigmentation intensity in NE-treated hair shafts compared to controls (Figure 2B), in alignment with the ectopic melanin redistribution seen in the upper epidermis (Figure 1C). Quantitative measurement of hair shaft blackness using ImageJ analysis confirmed a significant decrease in melanin content following NE exposure (Figure 2C, $p < 0.01$).

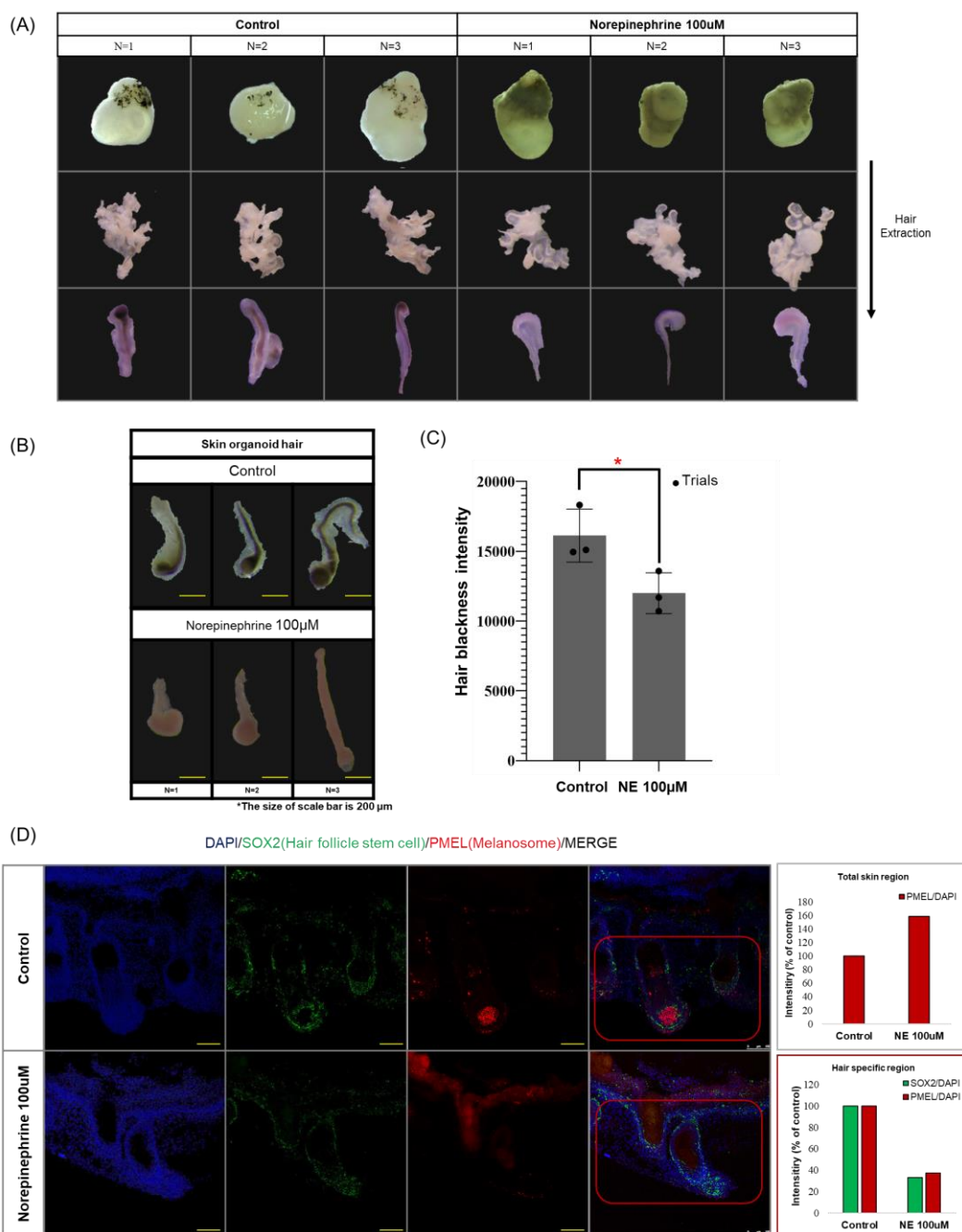


Figure 2. NE Treatment Reduces Melanin Content in Isolated Hair Shafts from Human Hairy Skin Organoids. (A) Sequential images showing the isolation procedure of hair shafts from organoid-associated tissue. Each step—from whole organoid, to separated hair-bearing tissue, to isolated hair shaft—is shown for control and NE (100 μ M)-treated groups ($n = 3$ per group). (B) Representative high-resolution images of individually isolated hair shafts from each group. Scale bar, 200 μ m. (C) Quantification of hair shaft pigmentation based on ImageJ analysis of hair blackness. Hair shafts from NE-treated organoids exhibited significantly reduced pigmentation compared to control. Each dot represents an independent trial; data are shown as mean \pm SEM. Statistical significance was determined by unpaired two-tailed t-test; ** $p < 0.01$. (D) Immunofluorescence analysis of hair follicle stem cells and melanosomes in hair-bearing regions and epidermis of hairy skin organoids. DAPI (blue, nuclei), SOX2 (green, hair follicle stem cells), and PMEL (red, melanosomes). Quantification (right panel) of SOX2 and PMEL were analyzed by Image J.

To further characterize changes in melanin distribution and stem cell niche integrity, we performed immunofluorescence staining using two key markers: SOX2, a transcription factor expressed in hair follicle stem cells [3], and PMEL, a melanosomal protein indicative of pigment granule presence [4]. Rather than focusing solely on expression levels, we examined spatial localization patterns of these markers to determine how stress impacts pigment positioning. In control organoids, SOX2⁺ cells were localized around the follicular bulb region, consistent with the presence of a maintained stem cell pool. PMEL signal was predominantly confined to areas adjacent to the hair shaft, indicative of properly localized melanosome activity. In contrast, NE-treated organoids showed a marked reduction in SOX2 signal, suggesting depletion of follicular stem cells. Moreover, PMEL staining shifted upward toward the suprabasal epidermis, reflecting mislocalized melanin granules and disrupted pigment homeostasis (Figure 2D). Quantification of fluorescence intensity confirmed significantly reduced SOX2 and PMEL expression in the follicular region, supporting the conclusion that NE not only depletes stem cells but also alters the spatial pattern of melanin deposition.

3.3 Construction of Single-Cell Transcriptomic Landscape in Hairy Skin Organoids

To validate the cellular heterogeneity and developmental fidelity of the human hairy skin organoid model, we performed scRNA-seq. UMAP-based clustering identified distinct cell populations, including melanocytes, basal keratinocytes, fibroblasts, confirming diverse lineage specification within the organoids (Figure 3A). The relative proportions of these cell types were visualized through stacked bar plots, further supporting robust differentiation (Figure 3B). To further explore lineage dynamics, pseudotime trajectory analysis was performed, resulting developmental trajectories captured continuous transitions across cell states, suggesting progressive cellular maturation within the organoid environment (Figure 3C–D). Additionally, the expression dynamics of key genes involved in extracellular matrix organization (e.g., COL1A2, COL6A1, LUM) and pigmentation (e.g., MITF, TYR, PMEL) were mapped along pseudotime (Figure 3E). The stage-specific and sequential activation of these markers confirms that our scRNA-seq dataset faithfully reflects the spatial and temporal gene regulation observed during human skin and follicle development.

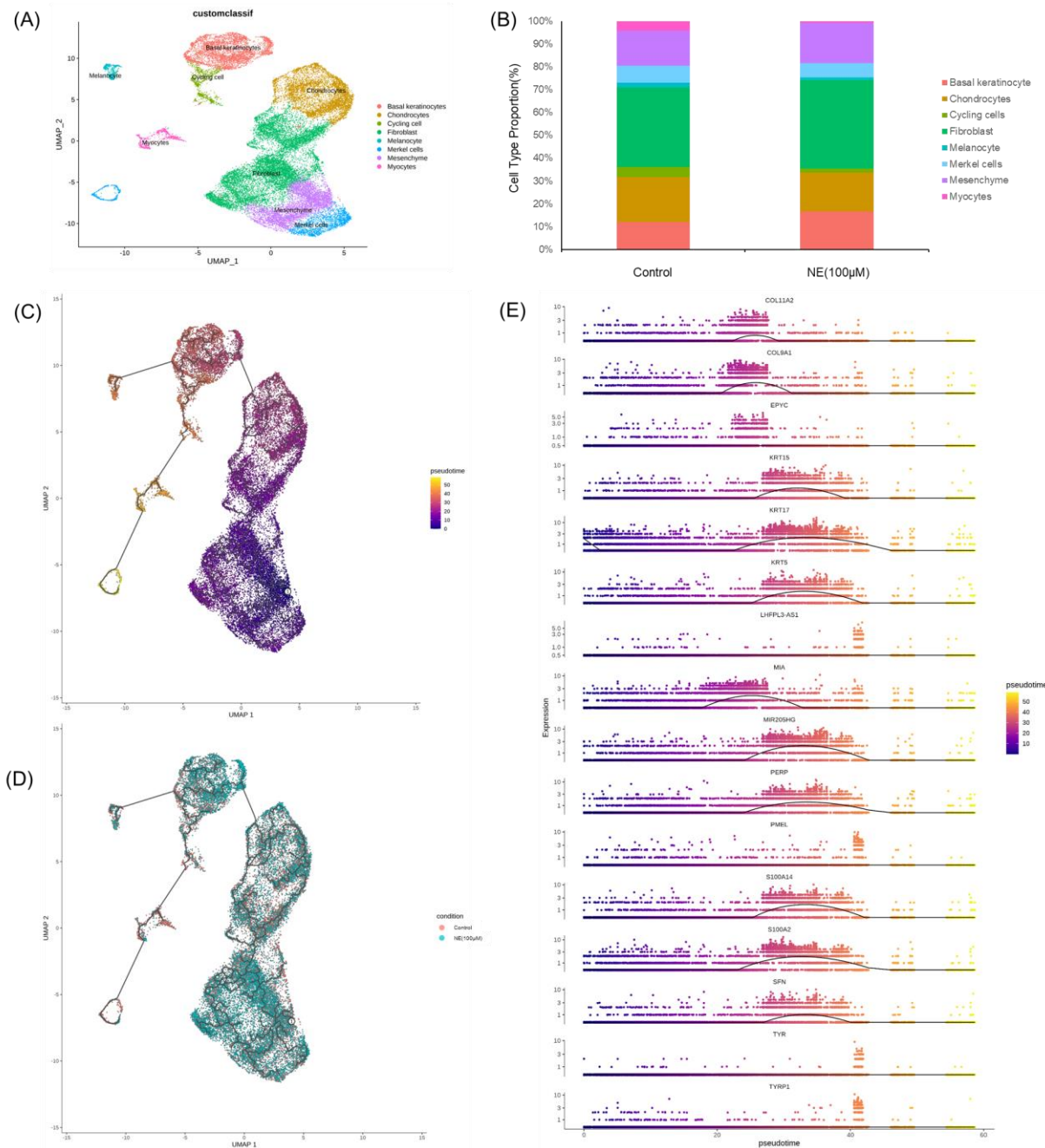


Figure 3. Single-cell transcriptomic analysis reveals NE-induced transcriptional trajectory shifts in human hairy skin organoids. (A) UMAP plot showing major cell populations annotated by customized markers. (B) Stacked bar graph comparing cell type proportions between control and NE-treated groups. (C) Pseudotime trajectory inferred across all cells using RNA velocity-based lineage inference. (D) Distribution of pseudotime values in control vs. NE-treated conditions. (E) Gene expression trends along pseudotime for ECM-related and pigmentation-related markers. Each dot represents a single cell, colored by pseudotime. LOESS-smoothed curves indicate gene expression dynamics across the pseudotime axis.

3.4 NE-Induced Remodeling of Cell-Cell Communication and Disruption of IGF and CADM Signaling Networks

To explore the molecular mechanisms underlying NE-induced pigmentation changes, we investigated cell–cell communication

151
152
153
154
155
156
157
158
159

160
161

162
163

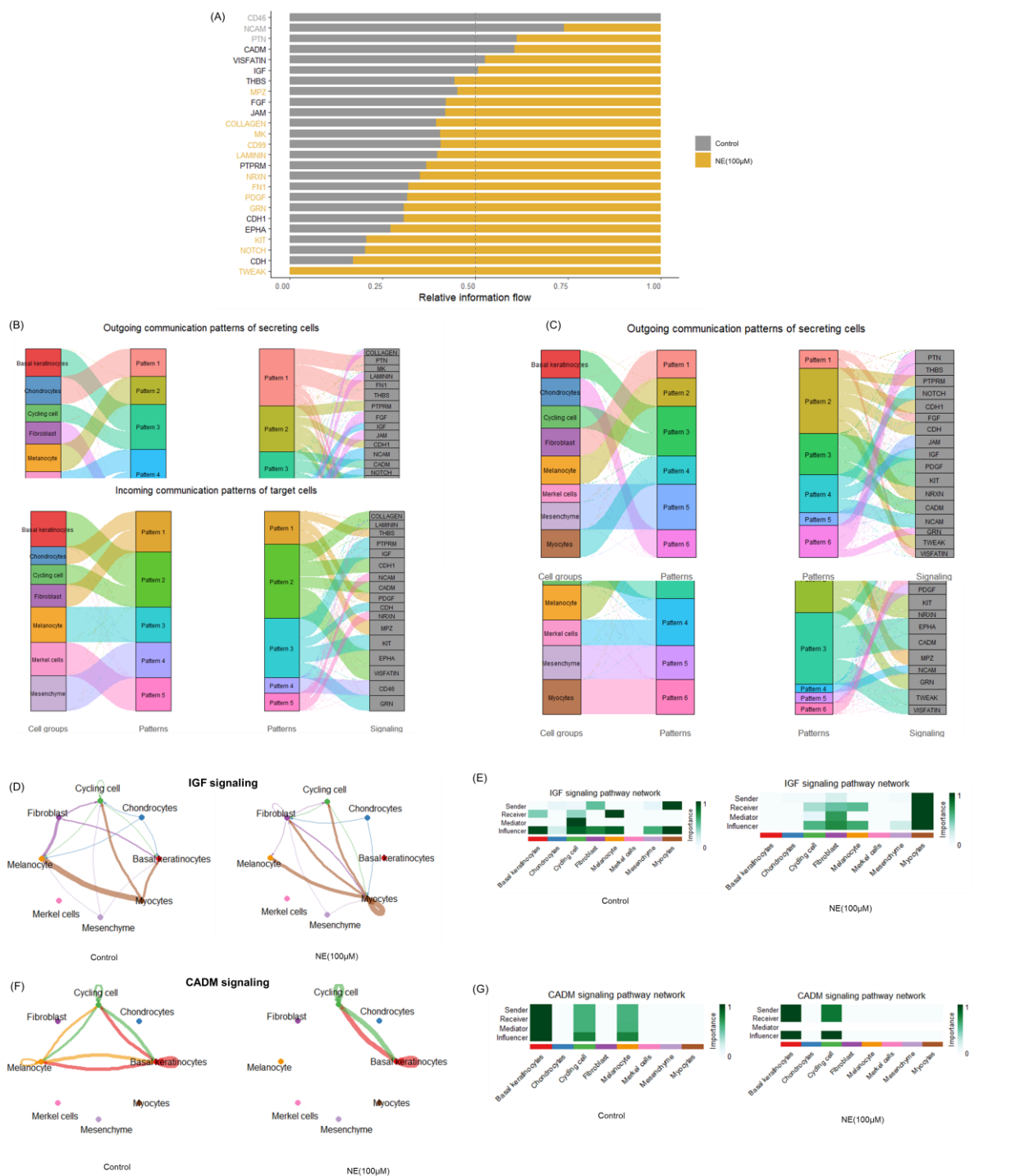


Figure 4. NE Exposure Modulates Intercellular Communication Dynamics and Alters IGF/CADM Signaling Pathways in Human Hairy Skin Organoids. (A) Comparison of key intercellular communication pathways between control (grey) and NE-treated (100 μ M) organoids. (B–C) Outgoing and incoming signaling patterns illustrate changes in pathway activity across cell populations. (D–E) IGF signaling networks and quantification reveal reduced interaction strength following NE treatment. (F–G) CADM signaling also shows diminished communication in NE-exposed organoids, particularly affecting communication between melanocytes and adjacent niche cells.

patterns using CellChat, a computational framework for modeling intercellular signaling based on scRNA-seq data [5]. Comparative analysis revealed that multiple signaling pathways were

164
165
166
167
168
169
170
171

172
173
174

differentially enriched between control and NE-treated human hairy skin organoids (Figure 4A). Notably, NE treatment resulted in a shift in both outgoing and incoming communication patterns, with distinct pathway clusters identified in secreting and receiving cell populations (Figure 4B–C).

Further dissection of individual pathways revealed specific disruptions in key signaling axes. The insulin-like growth factor (IGF) signaling network was markedly altered under NE treatment, as reflected by reduced interaction strength and connectivity among cell types (Figure 4D–E). Similarly, cell adhesion molecule (CADM) signaling exhibited a significant reduction in intercellular signaling density, particularly affecting communication between melanocytes and adjacent niche cells (Figure 4F–G).

3.5 NE Induces Distinct Transcriptional Alterations in Melanocytes

To further delineate the melanocyte-specific response to stress signaling, we performed differential gene expression analysis between control and NE-treated human hairy skin organoids.

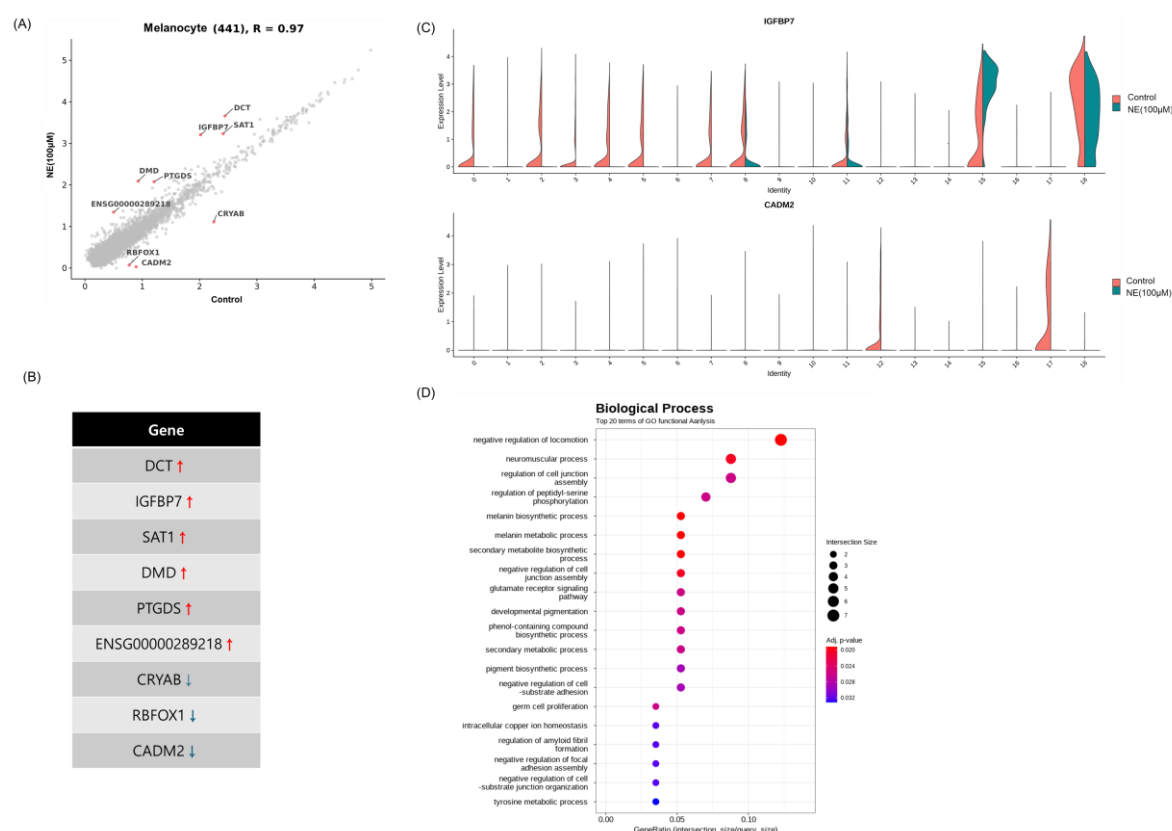


Figure 5. Differential Gene Expression and Functional Enrichment Analysis of Melanocytes Under NE Exposure. (A) Scatter plot comparing melanocyte gene expression between control and NE-treated organoids. (B) Table of top differentially expressed genes related to pigmentation, signaling, and stress response in melanocytes. (C) Violin plots of IGFBP7 (upregulated) and CADM2 (downregulated) in Cluster 15 melanocytes. (D) GO enrichment analysis showing top biological

175
176
177
178
179

180
181
182
183
184
185
186
187

188
189

190
191
192

193
194
195
196
197

processes affected by NE, with dot size and color indicating gene count and significance, respectively.	198
Scatter plot visualization of average gene expression in melanocytes revealed a strong correlation between conditions ($R = 0.97$), yet identified several genes with significant expression shifts following NE exposure (Figure 5A). These included upregulation of DCT, IGFBP7, SAT1, DMD, and PTGDS, as well as downregulation of CRYAB, RBFOX1, and CADM2, implicating changes in pigmentation, extracellular matrix signaling, and stress response pathways (Figure 5B).	199 200 201 202 203 204 205 206
To assess the cell-specific transcriptional changes, we analyzed gene expression across melanocyte clusters. Violin plots revealed that IGFBP7 was upregulated and CADM2 downregulated in Cluster 15 melanocytes, indicating heightened NE sensitivity (Figure 5C). Gene Ontology (GO) enrichment analysis supported these findings, with enriched terms related to melanin biosynthesis, cell adhesion, and tyrosine metabolism (Figure 5D). These data suggest that NE disrupts intercellular communication and induces intrinsic transcriptional alterations in melanocytes, contributing to pigment loss and mislocalization in stress-induced greying.	207 208 209 210 211 212 213 214 215 216 217
<i>4. Discussion</i>	218
4.1 Comparison to Previous Study—Previous investigations in murine models have demonstrated that stress-induced NE signaling promotes hair depigmentation through depletion of McSCs. However, analogous evidence in human systems has remained limited due to the lack of physiologically relevant platforms. Here, we established a hPSC-derived hairy skin organoid model that recapitulates NE-mediated pigmentary changes, offering mechanistic insights at single-cell resolution. This system enables precise investigation of melanocyte-specific and niche-related transcriptional responses to stress stimuli.	219 220 221 222 223 224 225 226 227 228
4.2 Plausible Mechanism—In our human organoid model, NE exposure induced premature activation of stem-like melanocytes, evidenced by increased expression of differentiation-related genes such as DCT and TYRP1. This aberrant activation likely drives ectopic pigmentation. Additionally, genes regulating melanosome localization and adhesion—CADM2 and IGFBP7—were significantly affected. CADM2, essential for anchoring melanosomes and maintaining melanocyte-keratinocyte contact [6], was downregulated, while IGFBP7 was upregulated, potentially disrupting IGF signaling and cellular homeostasis [7]. These transcriptional shifts may impair melanosome transfer and retention, contributing to pigment loss. Gene ontology analysis further supported this mechanism, highlighting pathways related to cell	229 230 231 232 233 234 235 236 237 238 239 240 241

junction assembly and reduced cellular motility—both of which are critical for correct melanosome positioning. 242
243

4.3 Limitation and Strength—Although the extended culture duration required for organoid maturation poses a limitation of this system, its biological fidelity and human specificity present significant advantages. This is the first study to reconstruct stress-induced hair greying in a human-derived organoid with integrated morphological and transcriptomic analysis. Moreover, the identification of IGFBP7 and CADM2 as potential regulatory nodes underscores the model's utility in elucidating stress-responsive pigmentation pathways. 244
245
246
247
248
249
250
251
252

5. Conclusion 253

This study presents a robust, human-relevant *in vitro* model for investigating the mechanisms of stress-induced hair greying. The hPSC-derived hairy skin organoid system offers a sustainable, ethically viable alternative to animal experimentation and advances the field of regenerative dermatology. In parallel with recent achievements such as POLA's award-winning "mirror skin" platform—an iPSC-based personalized skin model recognized at the 2024 IFSCC Congress—our work reinforces the translational potential of stem cell-derived organoids in personalized medicine and cosmetic science. Given current developmental trajectories, it is plausible that hair follicle organoids will serve as functional replacements for preclinical animal models within the next 1–2 years, enabling high-resolution, human-specific investigations of developmental biology. 254
255
256
257
258
259
260
261
262
263
264
265
266
267
268

References 268

- [1] Baumans, V. (2004). Use of animals in experimental research: an ethical dilemma?. *Gene therapy*, 11(1), S64-S66. 269
270
- [2] Zhang, B. et al. (2020). Hyperactivation of sympathetic nerves drives depletion of melanocyte stem cells. *Nature*, 577(7792), 676-681. 271
272
- [3] Laga, A. C. et al. (2010). Expression of the embryonic stem cell transcription factor SOX2 in human skin: relevance to melanocyte and merkel cell biology. *The American journal of pathology*, 176(2), 903-913. 273
274
275
- [4] Bissig, C. et al.. (2016). PMEL amyloid fibril formation: the bright steps of pigmentation. *International journal of molecular sciences*, 17(9), 1438. 276
277
- [5] Jin, S. et al. (2021). Inference and analysis of cell-cell communication using CellChat. *Nature communications*, 12(1), 1088. 278
279
- [6] Domingues, L. et al. (2020). Coupling of melanocyte signaling and mechanics by caveolae is required for human skin pigmentation. *Nature communications*, 11(1), 2988. 280
281
- [7] Evdokimova, V. et al. (2012). IGFBP7 binds to the IGF-1 receptor and blocks its activation by insulin-like growth factors. *Science signaling*, 5(255), ra92-ra92. 282
283